Journal of Membrane Science and Research 6 (2020) 218-225

Journal of Membrane Science & Research

journal homepage: www.msrjournal.com

Research Paper

Alkaline Stability of Novel Aminated Polyphenylene-Based Polymers in Bipolar Membranes

Rodrigo J. Martínez, Yingying Chen, Don Gervasio, James C. Baygents, James Farrell *

Department of Chemical and Environmental Engineering, University of Arizona, 1133 E. James E. Rogers Way, Tucson, AZ 85721 USA

Article info

Received 2019-10-09
Revised 2019-12-06
Accepted 2019-12-24
Available online 2019-12-24

Keywords

Bipolar membrane
Alkaline hydrolysis
Membrane degradation
Density functional theory
Poly(biphenyl alkylene)
Polysulfone

Highlights

- No increase in voltage for polyphenylene-based membranes under operating conditions.
- Commercial bipolar membranes showed 3-4 mV/d increases in operating voltage.
- DFT calculations and stability tests showed PBPA membrane was most stable.

Graphical abstract

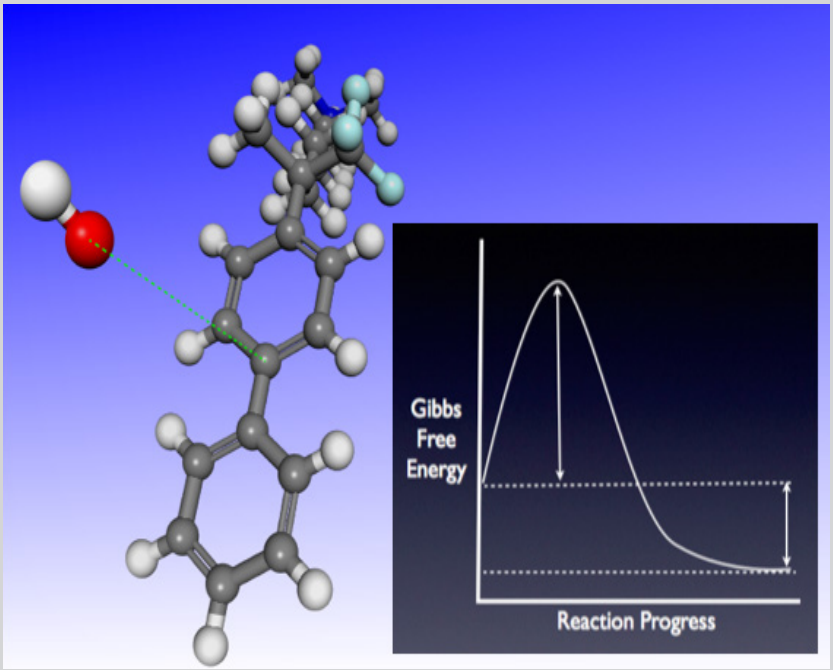

Abstract

This research investigated stability of two novel aminated polyphenylene polymers as anion exchange layers in bipolar membranes. Bipolar membrane stability was tested under operating conditions of 50 mA/cm^2, and under conditions of soaking in room temperature 1 M NaOH. The stability of the custom made bipolar membranes was compared with those for two commercial membranes. For the polyphenylene-based membranes, there was no measurable increase in operating voltage when run continuously at a current density of 50 mA/cm^2. For the two commercial membranes, the operating voltages increased by 3.2 to 4.4 mV per day when operated continuously over an 85 day testing period. Commercial membrane degradation in 1 M NaOH was similar to that under real operating conditions, with average rates of voltage increase of 3.2 to 3.5 mV/d. The custom made membrane containing a quaternary ammonium-tethered poly(biphenylalkylene) (PBPA) anion exchange layer did not show any loss in performance in either stability test. Density functional theory (DFT) simulations were used to calculate activation barriers and reaction energies for nucleophilic attack on the polymer backbones and cation functional groups on each of the four anion exchange polymers. Cation loss from all four polymers was thermodynamically favorable, with activation barriers ranging from 64 to 138 kJ/mol. The two commercial polysulfone-based anion exchange membranes were susceptible to cleavage of the ether bonds. However, the polyphenylene-based anion exchange polymers were considerably more stable with respect to backbone cleavage. The DFT calculations showing that the PBPA polymer was the most stable confirmed the results of the stability tests.

© 2020 MPRL. All rights reserved.

1. Introduction

Bipolar membranes (BPMs) are used to split water into H^+ and OH^- ions in a variety of industrial applications, including: production of mineral acids from salt solutions, recovery of organic acids from fermentation broths, pH control in biochemical processes, recovery and purification of pharmaceuticals, deacidification of fruit juices, and energy storage and conversion [1,2,3]. Despite their commercial availability since 1977, the use of bipolar membranes has been limited due to the low stability of the strong-base anion exchange membranes under alkaline conditions.

Bipolar membranes consist of a strong base anion exchange membrane laminated to a strong acid cation exchange membrane. The interface between the two membranes normally contains a weak base or weak acid catalyst to promote water splitting [4]. When placed in an electrodialysis cell,

* Corresponding author: farrellj@email.arizona.edu (J. Farrell)

DOI: 10.22079/JMSR.2019.115517.1298

polarization of the electrodes draws mobile counter ions out of the anion and cation exchange layers, leaving an ion depleted region between the two membranes. With increasing applied potential, there are insufficient mobile counter ions to carry the current, and water splitting commences at the interface between the two membranes. Nascent OH^- ions electromigrate and diffuse through the anion exchange membrane to produce a high pH solution, as illustrated in Figure S1 in the Supplementary Information. Likewise, H^+ ions are transported through the cation exchange membrane to produce an acid solution. Thus, normal operation of bipolar membranes expose the anion exchange layers to highly alkaline solutions. These conditions are suitable for a nucleophilic attack by hydroxide ions, either on the polymer backbone, or on the strong base cationic functional groups, both of which will adversely affect the membrane's dimensional stability and ionic conductivity [5,6].

The most commonly used anion exchange membranes contain benzyl-tethered trimethylammonium (TMA) cationic groups, due to their relative ease of synthesis and high alkaline stability [7]. One of the advantages of having the cationic group at the benzylic position is the absence of β-hydrogen atoms that allow for Hofmann elimination of the quaternary ammonium group [8]. However, the quaternary ammonium group attached at the benzylic position may not have sufficient stability for long-term use at high pH [9,10]. Previous studies have investigated the relative stability of different cationic functional groups [10]. One particularly stable cation found in commercial membranes is 1,4-diazabicyclo[2,2,2]octane (DABCO) [10,11,12]. The high stability of this diamine towards nucleophilic attack results from distributing the positive charge along the cyclic cation [12,13]. Other investigators have proposed that attachment of quaternary ammonium groups to the polymer backbone via a long alkyl side chain can reduce nucleophilic attack by hydroxide, thereby improving alkaline stability [14,15,16,17]. However, the mechanism for this increased stability is not understood.

Investigations of anion exchange membrane stability have also focused on polymer backbone degradation. Until recently, polystyrene cross-linked with divinylbenzene has been the most commonly used backbone for anion exchange membranes. Currently, polysulfone is the most commonly used backbone in commercial anion exchange membranes [18]. Polysulfones are considered state of the art in anion exchange membranes due to their high dimensional stability and resistance to acids, alkalis and oxidants [12,17]. However, under highly alkaline conditions, polysulfones have been observed to undergo hydrolysis, with the ether bonds the points of failure. To avoid this problem, polymer backbones without aryl-ether bonds have been developed. In alkaline fuel cell applications, aminated tetramethylpoly(phenylene) (ATMPP) and aminated poly(biphenylalkylene) (PBPA) polymers have shown relatively good mechanical and chemical stability [9,16,19].

The stability of anion exchange membranes under alkaline conditions is normally determined by exposing the membranes to concentrated alkali solutions at elevated temperatures. The membranes are then tested for changes in ion exchange capacity, area resistance, permselectivity, water content, and Young's modulus to assess polymer degradation. In addition, internal reflection FTIR and nuclear magnetic resonance can detect loss of functional groups if the membranes are sufficiently degraded [10]. In tests lasting several hours, Bauer et al. used immersion in 2 N KOH at 160 °C to assess anion exchange membrane stability [11]. In tests lasting one week, Hwang and Choi used 2.5 and 5 M NaOH solutions over a temperature range from 20 to 50 °C to determine the stability of a commercial bipolar membrane [20]. These short-term evaluations of membrane stability under very aggressive conditions are not as useful as stability tests under real use conditions. In addition, determining the relative stability of different functional groups is complicated when tests are performed on an entire membrane, due to differences in: polymer backbone composition, polymer entanglement and cross linking, molecular weight, polymer density, and testing procedures.

Quantum chemistry modeling can be used to compare the relative stabilities of different cationic functional groups and different polymer backbone structures without the complications associated with testing entire membranes. In addition, quantum chemistry modeling can be used to determine fundamental thermodynamic parameters that characterize polymer stability, without resorting to short-term testing under conditions that are more aggressive than actual use conditions.

The primary goal of this research was to investigate the stability of ATMPP and PBPA polymers as anion exchange layers in bipolar membranes. These two polymers have not previously been used in a bipolar membrane. A second goal of this research was to compare the stability of the laboratory synthesized bipolar membranes to two commercial bipolar membranes under actual working conditions. Towards that end, bipolar membrane electrodialysis experiments were conducted over periods of up 85 days of continuous operation at constant applied currents. Changes in voltage were monitored to assess degradation of the membranes. To compare bipolar membrane deterioration under working conditions to traditional testing procedures, bipolar membranes were also soaked in room temperature 1 M NaOH, and then tested over a 34-day period. Density functional theory (DFT) calculations were used to investigate the relative stability of the different cations and polymer backbones.

2. Materials and methods

2.1. Membrane materials

Two custom made bipolar membranes were prepared using Nafion 117 cation exchange membranes and poly(biphenylalkylene)trimethylammonium (PBPA) [10], and tetramethylpoly(phenylene) aminated with trimethylamine (ATMPP) [4] anion exchange layers. The PBPA and ATMPP were synthesized using the methods in references [16,21,19], and ionomer solutions were provided by Los Alamos National Laboratory (USA). Structures for the anion exchange polymers are shown in Figure 1, and a summary of the properties of the PBPA and ATMPP is given in Table 1. Before casting the ionomer solutions onto the Nafion membranes, the Nafion was treated following the method described in [22]. Nafion was immersed in 3% H_2O_2 at 80 °C for 1 hour, rinsed with deionized (DI) water, and then soaked in 1 M H_2SO_4 at 80 °C for 1 hour. The Nafion membrane was then rinsed with 80 °C DI water until free of acid. A graphene oxide catalyst layer was then spin-coated on the Nafion membrane at 500 rpm using 0.5 mL of an aqueous dispersion with a concentration of 5 g/L and flake size of 0.5-5 μm (Graphene Laboratories, Inc. Ronkonkoma, NY). The catalyst coated membrane was then dried at 100 °C for three minutes. The bipolar membrane was made by casting the anion exchange ionomer solution on top of the Nafion, which was placed on a vacuum table at room temperature. The bipolar membranes were dried overnight at room temperature. The thickness of the anion exchange layers in the custom membranes were ~75 μm. Custom membranes without the graphene oxide catalyst layer were also prepared.

Table 1
Properties of PBPA and ATMPP anion exchange membranes [23].

Ionomer	Ion Exchange Capacity (meq/g)	Water Uptake (%)	OH^- Conductivity (mS/cm)
PBPA	2.61	145	62
ATMPP	2.43	117	86

The two commercial bipolar membranes tested were Neosepta BP-1 from ASTOM Co., Japan and Fumasep FBM from FumaTech Co., Germany. These are the two most commonly used bipolar membranes in commercial applications. Neosepta BP-1 is composed of Neosepta CM-1 as the cation exchange layer, polysulfone aminated with trimethylamine as the anion exchange layer (PSF-TMA), and ferric hydroxide as the interlayer catalyst [24]. Fumasep FBM is composed of sulfonated crosslinked poly-ether ether ketone (PEEK) as the cation exchange layer, polysulfone with 1,4-diazabicyclo[2,2,2]octane (PSF-DABCO) [25] as the anion exchange layer, and polyacrylic acid/polyvinylpyridine as the catalyst [26]. The anion exchange polymer structures for the two commercial membranes are shown in Figure 1.

2.2. Stability testing

Bipolar membranes were tested in custom made electrochemical cells via recirculation of a 0.66 M Na_2SO_4 (ionic strength of 1 M) electrolyte solution at a flow rate of 10 ml/min in each chamber. The cells were operated at a constant current density of 50 mA/cm^2, which is a typical operating condition for bipolar membranes [1]. Rubber gasketing was used to make the effective area of each membrane 1 cm^2. The anode and cathode were both platinized titanium, and two custom Ag/AgCl reference electrodes were placed on each side of the bipolar membrane, as illustrated in Figure S2. A Sterilight SC1 UV sterilizer was connected in the recirculation loop to remove any persulfate produced at the anode. Potentiostats were used to record the voltages as a function of time. A second aging procedure involved soaking the bipolar membranes in 1 M NaOH at room temperature (~22 °C). The membranes were then periodically placed in an electrochemical cell to generate current-voltage curves after elapsed times of 1 to 34 days.

2.3. DFT simulations

DFT calculations were performed using the DMol3 [27,28] package in the Biovia Materials Studio 2018 modeling suite using a 72-cpu workstation. All simulations were unrestricted spin, all electron calculations using the Minnesota 2011 meta-GGA functional (M11-L) [20] and triple-numeric plus polarization basis sets (TNP) [29]. This functional was selected due to its high accuracy in calculating chemical reaction energies for a wide variety of reaction types, with a mean unsigned error of 9.0 kJ/mol [30]. Thermal smearing of 0.005 Ha was used to aid numerical convergence. Implicit solvation was included in all simulations using the polarizable continuum solvation model COSMO-ibs, with a dielectric constant of 78.4 [31]. The Fukui functions for nucleophilic attack (f^+) were calculated using the default parameters of the software [32].

Gibbs free energies of reaction (ΔG^0_{rxn}) and Gibbs free energies of activation (ΔG^0_{act}) were calculated for nucleophilic attack by hydroxide ions (OH^-) at different sites on the polymer fragments. Reactant energies were calculated at a stationary point having the OH^- approximately 10 Å away from the reaction site. Activation energies were calculated via optimization using the eigenvector following method on the structure with the maximum energy along the reaction coordinate, defined as the length of the bond that was formed or broken during each reaction. Frequency calculations were performed to verify energy minima and transition states, and to determine thermal corrections at 298.15 K.

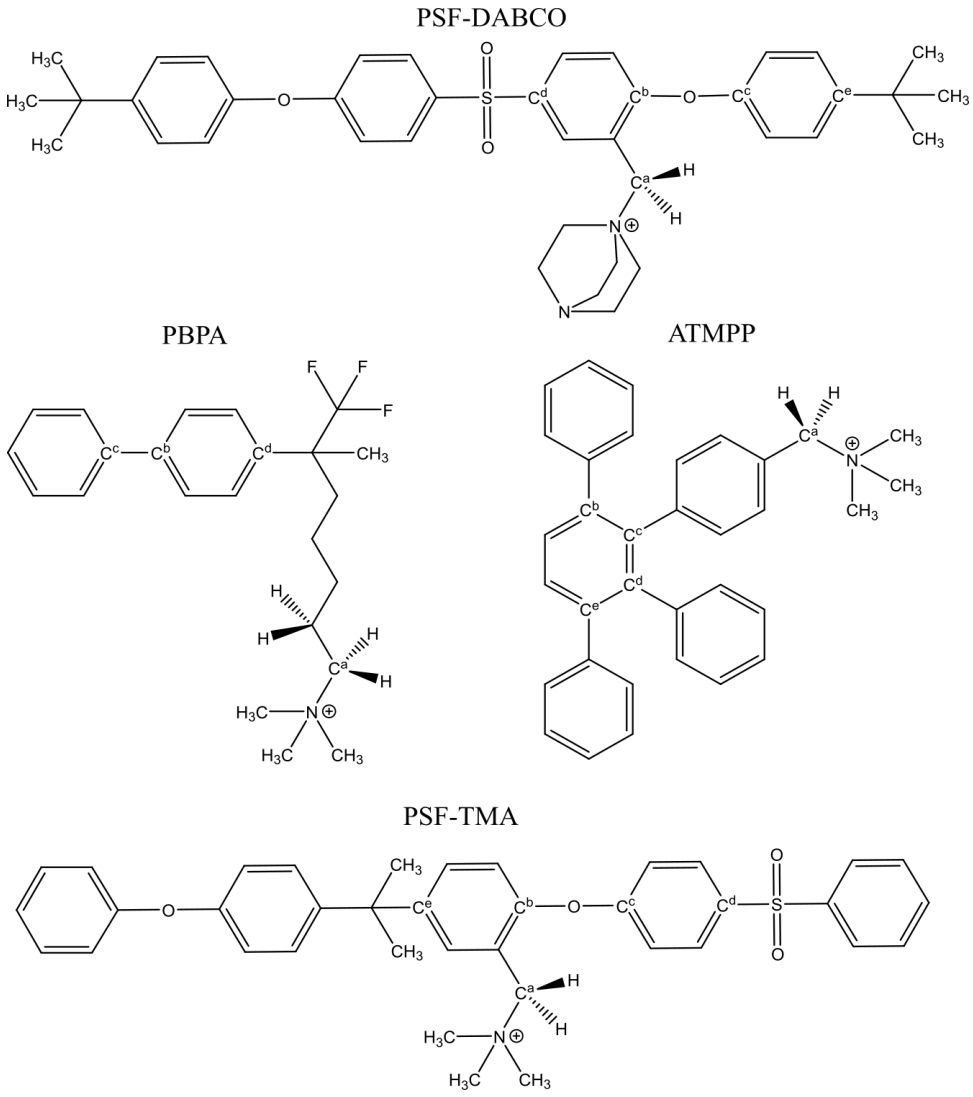

Fig. 1. Anion exchange polymers used in the bipolar membranes: polysulfone 1,4-diazabicyclo[2,2,2]octane (PSF-DABCO), polysulfone trimethylammonium (PSF-TMA), poly(biphenyl alkylene)trimethylammonium (PBPA), and ammoniumtrimethylpoly(phenylene) (ATMPP). C^a, C^b, C^d, C^e, H^b are for atom identification purposes.

3. Results and discussion

3.1. Stability tests

Measured voltages versus elapsed time of operation at 50 mA/cm^2 are shown for the four bipolar membranes in Figure 2. The voltages were continuously monitored via potentiostats recording voltages at 1 minute intervals. The data points in Figure 2 represent the average voltage over each 50-hour sampling period. Linear regressions to determine the rate of voltage increase are shown in Figure 2. The regression for the Fumasep membrane had the largest slope of 0.0044 V/d, followed by the Neosepta with 0.0032 V/d. In contrast, regressions for the PBPA and ATMPP membranes had negative slopes and low correlation coefficients. This indicates that there was no measurable increase in the operating voltages for the two custom made membranes.

Despite having the two most alkaline stable cations available in commercial membranes [10], both the Neosepta and Fumasep membranes showed performance declines over an 85-day period of operation. The declining performance of the membranes can likely be attributed to hydroxide attack on the cationic functional groups, and on the ether linkages in the

polysulfone polymer backbones. The data in Figure 2 are the first bipolar membrane stability tests conducted under operating conditions. Previous stability testing of the Neosepta membrane was conducted by soaking membranes in 2.5 and 5 M NaOH solutions at elevated temperatures [20]. Internal reflection FTIR spectroscopy showed loss of the TMA cations, but could not measure polymer backbone degradation.

The hydroxide ion concentrations in the anion exchange layers during bipolar membrane operation cannot be directly measured. However, numerical solutions of the Nernst-Plank equations for ion transport in bipolar membranes have shown that hydroxide ion concentrations in the anion exchange layer can be as great as 3 M at a current density of 50 mA/cm^2 [33]. Thus, although a neutral pH solution was fed into the testing cells, hydroxide ion concentrations inside the anion exchange layers most likely exceeded 1 M.

The second stability testing procedure involved soaking the bipolar membranes in 1 M NaOH for 34 days. Voltages versus elapsed time for the four membranes are shown in Figures S3-S6 for current densities ranging from 50 to 100 mA/cm^2. Over the 34-day testing period, the average rate of voltage increase was similar for the PSF-DABCO (0.0032 V/d), PSF-TMA (0.0035 V/d) and ATMPP (0.0036 V/d) bipolar membranes. However, the bipolar membrane with the PBPA anion exchange membrane did not show increasing voltage with elapsed time in 1 M NaOH. For that membrane, there was a decrease in operating voltage versus time at each current density. Thus, there was no measurable voltage increase for the bipolar membrane with PBPA anion exchange layer in either stability test.

3.2. DFT calculations

3.2.1 Cation Stability – Hydroxide Reactions with α-Carbon Atoms via SN2 Reaction

DFT modeling was used to determine the relative stability of the anion exchange layers of the four bipolar membranes. Detachment of the cationic functional group via a bimolecular nucleophilic substitution reaction (SN2) was examined for the PBPA, ATMP, PSF-TMA, and PSF-DABCO fragments shown in Figure 1. In this reaction mechanism, a hydroxide ion attacks the α-carbon atom, labeled as C^a in Figure 1. In the cases of PSF-TMA, PSF-DABCO and ATMPP, release of the cation via nucleophilic aromatic substitution was not examined because previous studies have shown that the phenyl-C^a bond is stronger than the N-C^a bond [16]. The nucleophilic substitution reactions produced a tertiary amine and a single bond between the hydroxide and the C^a atom on each fragment. All reactions yielded favorable Gibbs free energies of reaction, ranging from -66.5 kJ/mol to -107.5 kJ/mol, as illustrated in Figure 3. The activation energy barriers, ΔG^0_{act}, for these reactions were between 64.0 kJ/mol and 123.4 kJ/mol. The ATMPP and PSF-TMA structures with the TMA cation attached to the benzylic carbon atom yielded the lowest activation energies of 64.0 and 64.9 kJ/mol. The ΔG^0_{act} required for detaching the DABCO cation was 76.6 kJ/mol, which is ~12 kJ/mol higher than the energy barrier for PSF-TMA and ATMPP. This indicates that the DABCO cation is more kinetically stable than the TMA cation attached to the benzylic carbon atom. PBPA had the highest cation stability, with ΔG^0_{act} = 123.4 kJ/mol. This finding agrees with other studies showing that attaching the quaternary ammonium group to a polymer backbone with an alkyl spacer longer than three carbon atoms leads to an improved alkaline stability of the cation [9,15]. Although PBPA had the highest activation barrier for cation loss, it had the most favorable ΔG^0_{rxn} of all four polymer fragments.

Under normal operating conditions, the cationic sites in a bipolar membrane may have an adsorbed hydroxide ion, which will affect the stability of the cationic group. Thus, SN2 reactions were also modeled for the polymer fragments containing an adsorbed OH$^-$ ion. As shown in Table 2, hydroxide adsorption was energetically favorable on all cations, yielding free energies of reaction between -27.6 kJ/mol and -40.6 kJ/mol with no activation barriers. For the TMA containing polymers, the O-N distances for the adsorbed hydroxide ranged between 3.261 Å and 3.292 Å. In the case of the DABCO cation, the O-N distance to the closest nitrogen atom was 3.167 Å. This shorter distance is consistent with the more favorable ΔG^0_{rxn} for hydroxide adsorption on the DABCO cation.

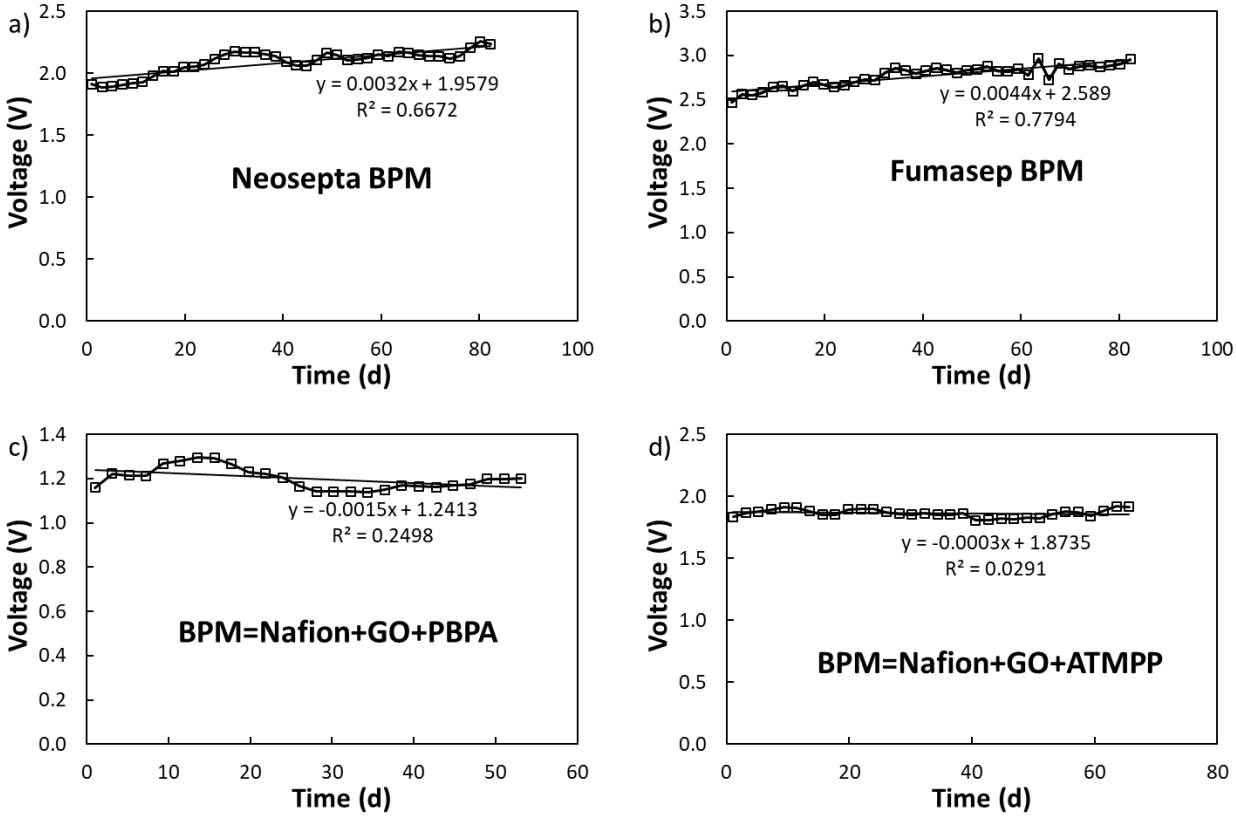

Fig. 2. Operating voltage versus elapsed time of operation at 50 mA/cm^2 for the commercial and custom made bipolar membranes (BPM). Linear regression parameters and correlation coefficients (R^2) are given for each data set.

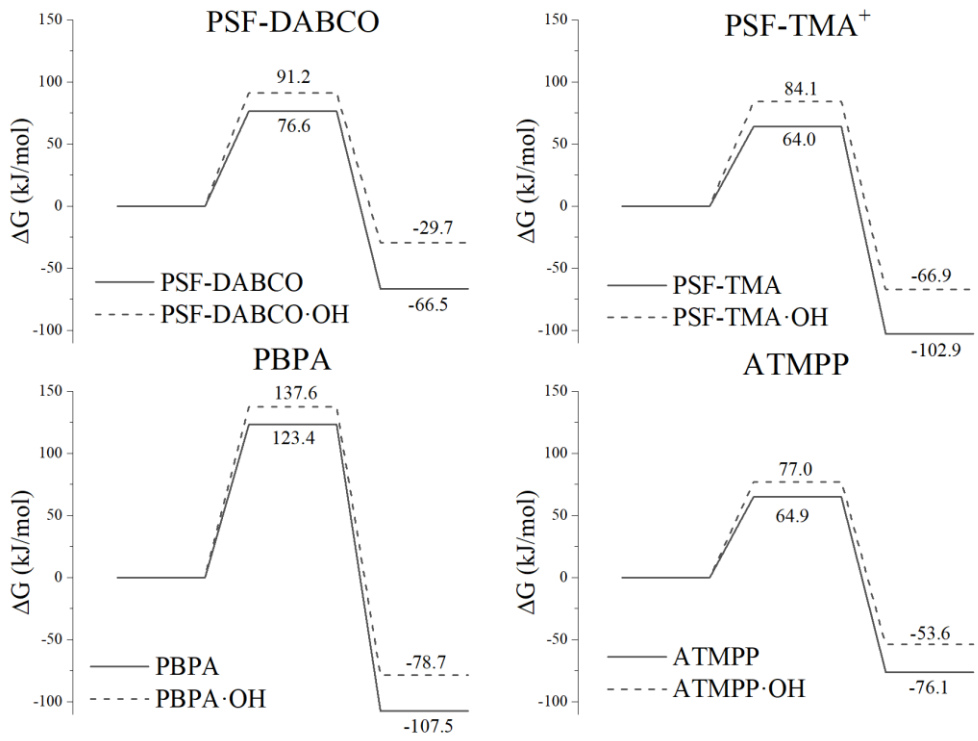

Fig. 3. Energy profiles for nucleophilic substitution of the cation. Solid lines represent the reaction without an adsorbed hydroxide ion, dashed lines represent the reaction with an adsorbed hydroxide ion.

In all cases, adsorption of the hydroxide ion reduced the C^a-N bond lengths, and decreased the Hirshfeld charges [34] on the C^a atoms, as shown in Table 2. This indicates a stronger bond and decreased electrophilicity of the C^a atom, which are reflected in lower Fukui f^+ indices that measure the local susceptibility to nucleophilic attack. With an adsorbed hydroxide ion, the energetic favorability for the SN2 reactions were lower by 22.5 to 36 kJ/mol. This is consistent with the shorter C^a-N bond lengths and decreased positive charge on the C^a atoms. Consistent with adsorbed hydroxide increasing the stability of cation, the activation energies for cation loss increased by 12.1 to 20.1 kJ/mol with adsorbed hydroxide.

3.2.2. Cation stability - Hofmann elimination via abstraction of β-hydrogen atoms

For the PBPA polymer, cation loss via Hofmann elimination (E2) is possible due to the β-hydrogen atoms on the C atom adjacent to C^a. In the cases of ATMPP, PSF-TMA, and PSF-DABCO, the cation is attached to a benzylic carbon atom, and Hofmann elimination cannot occur. Hofmann elimination was studied via abstracting the H□ atom on PBPA in Figure 4 with a hydroxide ion. This abstraction resulted in the release of trimethylamine and formation of a double bond between the β- and the α-carbon atoms.

The reaction energy profile in Figure 4 shows that Hofmann elimination was thermodynamically favorable, with ΔG^0_{rxn} = -107.5 kJ/mol and ΔG^0_{act} = 104.6 kJ/mol. The ΔG^0_{rxn} was less than 4 kJ/mol less negative than the nucleophilic substitution, and the activation energy was 18.8 kJ/mol lower than the SN2 reaction. Thus, the Hofmann elimination reaction is favored over the SN2 reaction for PBPA. However, the ΔG^0_{act} for cation loss via this reaction was 28.0 to 40.6 kJ/mol greater than that for the other three polymers, indicating that the PBPA has the most kinetically stable cation.

3.2.3. Polymer backbone stability - Cleavage of aryl-ether bonds

Ether hydrolysis of the polysulfone backbones on PSF-DABCO and PSF-TMA was examined via hydroxide attack on one of the carbon atoms in the ether group. The aryl-ether cleavage is considered a nucleophilic aromatic substitution reaction (SNAr). The carbon atom most susceptible to nucleophilic attack was determined from the Fukui f^+ indices, listed in Table 3. For both polysulfones, the highest f^+ index was on the carbon atom closest to the cation, and is represented as C^b in Figure 1. Both polymer backbones reacted with hydroxide via a two-step pathway, illustrated in Figure 5. The first step involved bonding of the OH^- to the C^b atom to form a Meisenheimer complex [35], with energy barriers of 33.6 and 42.2 kJ/mol. For PSF-TMA, complex formation was endergonic, with ΔG^0_{rxn} = 13.8 kJ/mol, whereas for PSF-DABCO, complex formation was exergonic, with ΔG^0_{rxn} = -19.8 kJ/mol. Both Meisenheimer complexes were stable, with ΔG^0_{act} barriers of 97.7 and 117 kJ/mol to cleave the aryl-ether bond. For the two-step process, the overall reactions were exergonic, with ΔG^0_{rxn} values of -123.4 kJ/mol (PSF-DABCO) and -101.0 kJ/mol (PSF-TMA). Final products of the aryl-ether cleavage reactions are shown in Figure S7 in the Supplementary Information. Although cleavage of the aryl-ether bonds was highly exergonic and more energetically favorable than for cation loss, the activation barriers for polymer backbone degradation were 20.6 to 27.4 kJ/mol greater than that for cation loss.

3.2.4. Polymer backbone stability - Cleavage of aryl-aryl bonds

Figure 6 shows the energy profiles for backbone degradation of PBPA and ATMPP via nucleophilic aromatic substitution. The most favorable location for nucleophilic attack on PBPA and ATMPP by OH^- was at C^b (Figure 1), which had the highest f^+ values (see Table 3). The attack broke the aryl-aryl bond of the backbone yielding a phenyl group and a phenoxide group. In both cases, the backbone degradation occurred via a three step sequence. First, the OH^- attached to the C^b atom with barrier heights of 88.3 kJ/mol (ATMPP) and 70.9 kJ/mol (PBPA), resulting in Meisenheimer complexes. Formation of both Meisenheimer complexes were exergonic, with ΔG^0_{rxn} values of 52.1 and 87.1 kJ/mol for ATMPP and PBPA, respectively. The ATMPP Meisenheimer complex was more stable than that for PBPA and had an activation barrier of 18.8 kJ/mol to revert back to the original reactants. For PBPA, there was only a 1.2 kJ/mol activation barrier for reversion to the reactants. Cleavage of the aryl-aryl bond from the Meisenheimer complexes had high activation barriers, for PBPA, ΔG^0_{act} =

215.6 kJ/mol and for ATMPP, ΔG^0_{act} = 220.9 kJ/mol. The cleavage formed a phenol, with the hydroxyl attached to the C^b atom, and an unstable phenyl anion. The phenyl anion then reacted with the phenolic H atom without an activation barrier to form the products shown in Figure S8. The overall reaction sequence for the both ATMPP and PBPA were not thermodynamically favorable for cleavage of the aryl-aryl bond. Furthermore, the high activation barriers for breaking the aryl-aryl bonds and the low barriers for reversion to the reactants from the Meisenheimer complexes indicates that this reaction mechanism will not significantly contribute to polymer degradation.

Table 2
C^a-N bond length, Hirshfeld charge on the C^a atom, and Fukui index for nucleophilic attack (f^+) on the C^a atom. Positive (+) refers to the cation without adsorbed hydroxide and OH^- adsorbed refers to the cation with an adsorbed hydroxide ion.

	ΔG^0_{rxn} (kJ/mol)	
PSF-DABCO	-40.6	
PSF-TMA	-34.6	
ATMPP	-28.6	
PBPA	-27.6	
	C^a-N length (Å)	
	Positive (+)	**OH^- adsorbed**
PSF-DABCO	1.462	1.459
PSF-TMA	1.493	1.484
ATMPP	1.492	1.485
PBPA	1.492	1.485
	C^a Hirshfeld charge	
	Positive (+)	**OH^- adsorbed**
PSF-DABCO	0.0191	0.0055
PSF-TMA	0.0259	0.0234
ATMPP	0.0278	0.0244
PBPA	0.0326	0.0291
	C^a f^+ index	
	Positive (+)	**OH^- adsorbed**
PSF-DABCO	0.010	0.008
PSF-TMA	0.008	0.006
ATMPP	0.010	0.008
PBPA	0.001	0.001

4. Conclusions

This research showed that there is measurable performance decline in bipolar membranes under real operating conditions over a time span of less than 90 days. The performance decline from soaking in 1 M NaOH at room temperature indicates that hydroxide concentrations greater than 1 M and elevated temperatures are not required to observe membrane degradation over a short time period. The two commercial polysulfone-based membranes showed measurable performance decline in both stability tests. For these membranes, the rates of voltage increase while operating at 50 mA/cm^2 were similar to those resulting from soaking in 1 M NaOH. The two custom membranes did not show measurable wear when operated continuously at 50 mA/cm^2. However, the ATMPP membrane did show increasing voltage over time after soaking in 1 M NaOH. Only the PBPA membrane did not show measurable degradation in both tests.

The DFT calculated activation barriers and reaction energies can only be considered approximations, since the polymer fragments modeled in the reactions do not have the steric restrictions that would likely be present in a real membrane phase. However, the calculations are useful for comparing the relative stability of different functional groups towards nucleophilic attack. Cation loss from all four anion exchange polymers was thermodynamically favorable, with ΔG^0_{rxn} values ranging from -29.7 to -107.5 kJ/mol. Activation barriers for loss of the TMA cation were as low as 64.0 kJ/mol. For the most stable PBPA membrane, the lowest activation barrier for cation loss was 28 to 40.6 kJ/mol greater than those for the other three polymers. Cleavage of the aryl-ether bonds in the commercial polysulfone membranes was thermodynamically favorable, with ΔG^0_{rxn} values more exergonic than -100 kJ/mol. However, the activation barriers for breaking the ether bonds were greater than those for cation loss. For the two custom made membranes, the polymer backbones were thermodynamically stable, with positive ΔG^0_{rxn} values and high activation barriers for aryl-aryl bond cleavage. Thus, the modeling results are in agreement with the stability tests showing PBPA as the most stable membrane.

Acknowledgements

This research was supported by the National Science Foundation Chemical, Bioengineering, Environmental and Transport Systems (CBET) Division through Grant #1604857, and by a fellowship from Consejo Nacional de Ciencia y Tecnología (CONACYT), Mexico to Rodrigo J. Martinez through Grant #409178. Thanks to Dr. Yu Seung Kim at Los Alamos National Laboratories for providing the ionomer solutions. Funding sources had no role in the research activities or in the preparation of this manuscript.

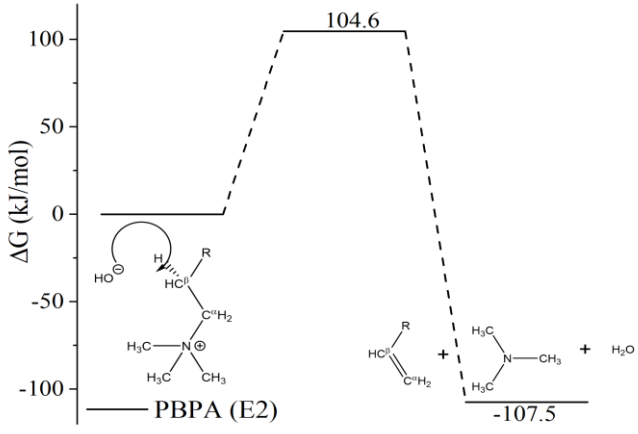

Fig. 4. Energy profile for Hofmann elimination (E2) in PBPA, the structures represent the elimination mechanism of the quaternary amine.

Table 3
Fukui function indices for nucleophilic attack (f^+), labels correspond to the carbon atoms in Figure 1.

	PSF-DABCO	PSF-TMA	ATMPP	PBPA
C^b	0.076	0.016	0.040	0.063
C^c	0.003	0.013	0.025	0.056
C^d	0.059	0.015	0.025	0.060
C^e	0.009	0.013	0.036	----

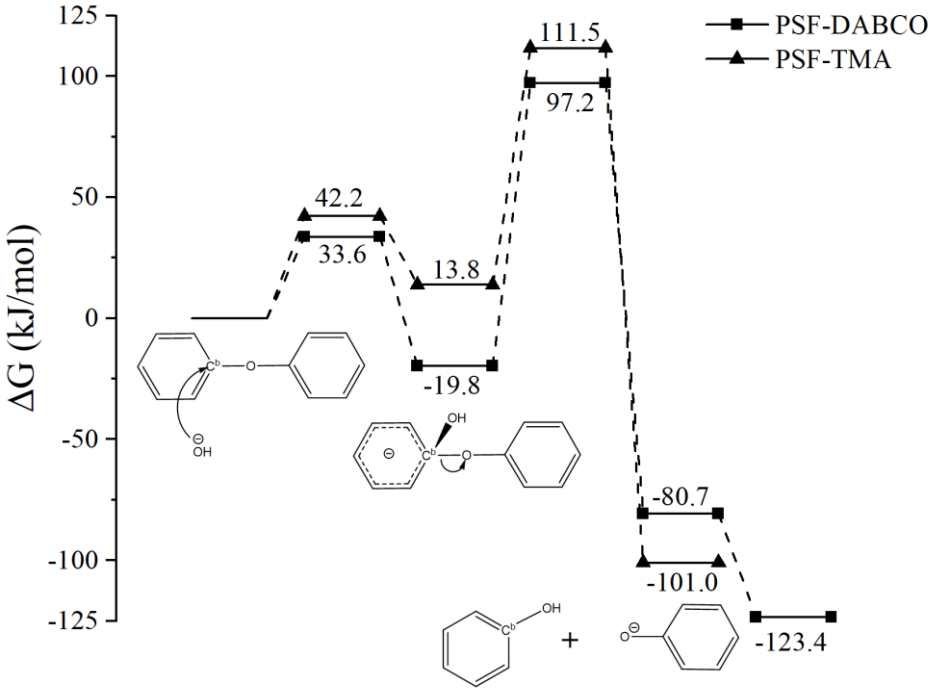

Fig. 5. Energy profile for breaking the aryl-ether bond in PSF-DABCO and PSF-TMA, the structures represent the cleavage mechanism of the aryl-ether bond.

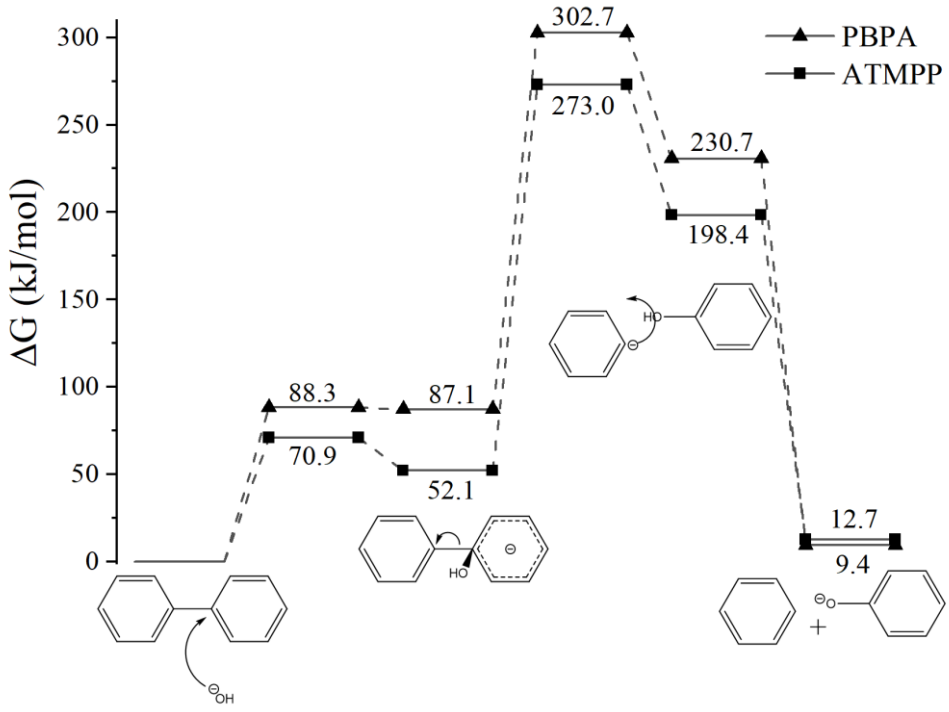

Fig. 6. Energy profiles for breaking the aryl-aryl bond in PBPA and ATMPP, the structures represent the cleavage mechanism of the aryl-aryl bond.

5. References

[1] H. Strathmann, Ion-Exchange Membrane Separation Processes, Elsevier, New York, 2004.

[2] M.B. McDonald, J.P. Bruce, K. McEleney, M.S. Freund, Reduced graphene oxide bipolar membranes for integrated solar water splitting in optimal pH, ChemSusChem. 8 (2015) 2645–2654. doi:10.1002/cssc.201500538.

[3] M.B. McDonald, M.S. Freund, P.T. Hammond, Catalytic, conductive bipolar membrane interfaces through layer-by-layer deposition for the

design of membrane-integrated artificial photosynthesis systems, ChemSusChem. 10 (2017) 4599–4609. doi:10.1002/cssc.201701397.

[4] R. Simons, Electric field effects on proton transfer between ionizable groups and water in ion exchange membranes, Electrochim. Acta. 29 (1984) 151–158.

[5] T. Sata, M. Tsujimoto, T. Yamaguchi, K. Matsusaki, Change of anion exchange membranes in an aqueous sodium hydroxide solution at high temperature, J. Memb. Sci. 112 (1996) 161–170. doi:10.1016/0376-7388(95)00292-8.

[6] C. Fujimoto, D.-S. Kim, M. Hibbs, D. Wrobleski, Y.S. Kim, Backbone stability of quaternized polyaromatics for alkaline membrane fuel cells, J. Memb. Sci. 423–424 (2012) 438–449. doi:10.1016/J.MEMSCI.2012.08.045.

[7] G. Merle, M. Wessling, K. Nijmeijer, Anion exchange membranes for alkaline fuel cells: A review, J. Memb. Sci. 377 (2011) 1–35. doi:10.1016/J.MEMSCI.2011.04.043.

[8] A.W. Hofmann, Research into the molecular constitution of the organic bases, Philosophical Transactions of the Royal Society of London. 141 (1851) 357–398. doi:10.1098/rstl.1851.0017

[9] M.R. Hibbs, Alkaline stability of poly(phenylene)-based anion exchange membranes with various cations, J. Polym. Sci. Part B Polym. Phys. 51 (2013) 1736–1742. doi:10.1002/polb.23149.

[10] A.D. Mohanty, C. Bae, Mechanistic analysis of ammonium cation stability for alkaline exchange membrane fuel cells, J. Mater. Chem. A. 2 (2014) 17314–17320. doi:10.1039/C4TA03300K.

[11] B. Bauer, H. Strathmann, F. Effenberger, Anion-exchange membranes with improved alkaline stability, Desalination. 79 (1990) 125–144. doi:10.1016/0011-9164(90)85002-R.

[12] M.L. Di Vona, R. Narducci, L. Pasquini, K. Pelzer, P. Knauth, Anion-conducting ionomers: Study of type of functionalizing amine and macromolecular cross-linking, Int. J. Hydrogen Energy. 39 (2014) 14039–14049. doi:10.1016/J.IJHYDENE.2014.06.166.

[13] J. Hnát, M. Plevová, J. Žitka, M. Paidar, K. Bouzek, Anion-selective materials with 1,4-diazabicyclo[2.2.2]octane functional groups for advanced alkaline water electrolysis, Electrochim. Acta. 248 (2017) 547–555. doi:10.1016/J.ELECTACTA.2017.07.165.

[14] M. Zhang, J. Liu, Y. Wang, L. An, M.D. Guiver, N. Li, Highly stable anion exchange membranes based on quaternized polypropylene, J. Mater. Chem. A. 3 (2015) 12284–12296. doi:10.1039/C5TA01420D.

[15] S. Chempath, J.M. Boncella, L.R. Pratt, N. Henson, B.S. Pivovar, Density functional theory study of degradation of tetraalkylammonium hydroxides, J. Phys. Chem. C. 114 (2010) 11977–11983. doi:10.1021/jp9122198.

[16] M.R. Hibbs, C.H. Fujimoto, C.J. Cornelius, Synthesis and characterization of poly(phenylene)-based anion exchange membranes for alkaline fuel cells, Macromolecules. 42 (2009) 8316–8321. doi:10.1021/ma901538c.

[17] G. Couture, A. Alaaeddine, F. Boschet, B. Ameduri, Polymeric materials as anion-exchange membranes for alkaline fuel cells, Prog. Polym. Sci. 36 (2011) 1521–1557. doi:10.1016/J.PROGPOLYMSCI.2011.04.004.

[18] A.D. Mohanty, C.Y. Ryu, Y.S. Kim, C. Bae, Stable eleastomeric anion exchange membranes based on quaternernary ammonium-tethered polystyrene-b-poly(ethylene-co-butylene)-b-polystyrene triblock copolymers, Macromol. 48 (2015) 7085-7095. doi:10.1021/acsmacromol.5b01382.

[19] W.-H. Lee, Y.S. Kim, C. Bae, Robust hydroxide ion conducting poly(biphenyl alkylene)s for alkaline fuel cell membranes, ACS Macro Lett. 4 (2015) 814–818. doi:10.1021/acsmacrolett.5b00375.

[20] Hwang, U.-S., J.-H. Choi. Changes in the electrochemical characteristics of a bipolar membrane immersed in high concentration of alkaline solutions, Sep. Pur. Tech. 48.1 (2006) 16-23.

[21] M.R. Hibbs, C.J. Cornelius, C.H. Fujimoto, Poly(phenylene)-based anion exchange membrane, U.S. Patent 7,888,397, February 15, 2011.

[22] F. Damay, L.C. Klein. Transport properties of Nafion™ composite membranes for proton-exchange membranes fuel cells, Solid State Ionics162 (2003) 261-267.

[23] M.R. Hibbs, Alkaline stability of poly (phenylene)-based anion exchange membranes with various cations, J. Polymer Sci. B: Polymer Phys. 51.24 (2013) 1736-1742.

[24] H. Fumio, K. Hirayama, N. Ohmura, S. Tanaka, Bipolar membrane and method for its production, U.S. Patent 5,221,455, June 22, 1993.

[25] F.G. Wilhelm, Bipolar membrane electrodialysis, University of Twente (2001).

[26] A. Kemperman, Handbook on Bipolar Membrane Technology, Twente University Press, Enschede, The Netherlands, 2000.

[27] B. Delley, An all-electron numerical method for solving the local density functional for polyatomic molecules, J. Chem. Phys. 92 (1990) 508. doi:10.1063/1.458452.

[28] B. Delley, From molecules to solids with the DMol3 approach, J. Chem. Phys. 113 (2000) 7756–7764. doi:10.1063/1.1316015.

[29] B. Delley, Fast Calculation of electrostatics in crystals and large molecules, J. Phys. Chem. 100 (1996) 6107–6110. doi:10.1021/jp952713n.

[30] R. Peverati, D.G. Truhlar, Improving the accuracy of hybrid meta-GGA density functionals by range separation, J. Phys. Chem. Lett. 2 (2011) 2810–2817. doi:10.1021/jz201170d.

[31] B. Delley, The conductor-like screening model for polymers and surfaces, Mol. Simul. 32 (2006) 117–123. doi:10.1080/08927020600589684.

[32] G. Fitzgerald, On the use of fractional charges for computing Fukui functions, Mol. Simul. 34 (2008) 931–936. doi:10.1080/08927020802073065.

[33] Y. Chen, Experimental and Theoretical Investigation of Electrochemical Water Treatment Processes, Doctoral Dissertation, University of Arizona, 2018.

[34] F.L. Hirshfeld, Bonded-atom fragments for describing molecular charge densities, Theor. Chim. Acta B 44 (1977) 129-138.

[35] F. Terrier, Rate and equilibrium studies in Jackson-Meisenheimer complexes, Chem. Rev. 82(2) (1982) 77–152. doi: 10.1021/cr00048a001.